Inverse Cascade Regime in Shell Models of Two-Dimensional Turbulence

Thomas Gilbert, Victor S. L'vov, Anna Pomyalov, and Itamar Procaccia
Department of Chemical Physics, The Weizmann Institute of Science, Rehovot 76100, Israel
(Received 11 January 2002; published 29 July 2002)

We consider shell models that display an inverse energy cascade similar to two-dimensional turbulence (together with a direct cascade of an enstrophylike invariant). Previous attempts to construct such models ended negatively, stating that shell models give rise to a ''quasiequilibrium'' situation with equipartition of the energy among the shells. We show analytically that the quasiequilibrium state predicts its own disappearance upon changing the model parameters in favor of the establishment of an inverse cascade regime with Kolmogorov scaling. The latter regime is found where predicted, offering a useful model to study inverse cascades.

DOI: 10.1103/PhysRevLett.89.074501 PACS numbers: 47.27.Gs, 05.45.–a, 47.27.Jv

The inverse energy cascade in two-dimensional Navier-Stokes turbulence is an important phenomenon with implications for geophysical flows [1]. In addition, it had been found that correlation functions and structure functions obey very closely Kolmogorov scaling (so-called K41), with only minute anomalous corrections, in contradistinction to three-dimensional turbulence in which intermittency corrections to K41 scaling are sizable [2]. This difference is well documented [3–5] but not yet understood. Also, experiments and simulations [2,5] indicate that the velocity distribution functions are very close to Gaussian, as if the system were very close to equilibrium, in apparent contradiction with the K41 scaling. It is therefore tempting to construct simple models of the phenomenon. Indeed, several attempts were made to construct shell models for this purpose [6,7]. So far, these attempts have ended negatively, failing to find a statistical steady state in which energy flows from smaller to larger scales *together* with having a Kolmogorov energy spectrum. Rather, it was thought that whenever energy flew ''backwards,'' the statistical steady state settled close to thermodynamic equilibrium. In this Letter we show that there actually exists a wide range of parameter values for which shell models display the required behavior, thereby offering useful testing grounds for ideas on two-dimensional turbulence. We also find that K41 scaling appears close to parameter values in which the system is in quasiequilibrium, offering interesting connections to two-dimensional turbulence.

We discuss the issue in the framework of the Sabra shell model [8]. Like all shell models [9] this represents a truncated Fourier representation of the Navier-Stokes equations. The Sabra model reads

$$\frac{du_n}{dt} = i(ak_{n+1}u^*_{n+1}u_{n+2} + bk_n u^*_{n-1}u_{n+1} - ck_n u_{n-1}u_{n-2}) - \gamma_n u_n + f_n, \qquad (1)$$

where the dissipative term γ_n reads $\nu k_n^{2\alpha} + \mu k_n^{-2\beta}$, with ν and μ being the viscosity and drag coefficients, respectively. Here u_n are complex numbers standing for the Fourier components of the velocity field belonging to shell n, associated with wave numbers k_n. The latter are restricted to the set $k_n = k_0\lambda^n$, with λ being the spacing parameter, taken below to be 2. The forcing f_n is chosen here to act at intermediate values of n, $n = n_f$, allowing one in principle to study direct as well as inverse fluxes. The forcing is taken random with Gaussian time correlations as in [8]; the amplitude of the forcing is fixed below to $1/\sqrt{2}$ in all cases. The dissipative terms γ_n act both on the smallest and the largest scales with their respective (hyper)-viscosity and drag exponents α and β; below we use $\alpha = \beta = 2$. The dissipative terms become dominant at the viscous and drag scales n_d and n_L, respectively. We will always have $n_L \ll n_f \ll n_d$. The coefficients a, b, and c are adjustable parameters, with the constraint $a + b + c = 0$ ensuring the conservation of energy in the dissipationless limit. Choosing $a = 1$ we explore the problem in terms of the single parameter b, with $-2 < b < 0$ [8].

It was shown before [10,11] that for $-2 < b < -1$ there exist two distinct positive definite invariants, the energy E and the ''enstrophy'' H,

$$E = \frac{1}{2}\sum_{n=1}^{N} |u_n|^2, \qquad H = \frac{1}{2}\sum_{n=1}^{N}\left(\frac{-1}{b+1}\right)^n |u_n|^2, \qquad (2)$$

which, in this case, are associated with an inverse and direct fluxes, respectively [6]. However, the statistical steady state found in the regime $-5/4 < b < -1$ in [6,7] is close to thermodynamic equilibrium. This can be demonstrated via the properties of the structure functions, defined by

$$S_2(k_n) = \langle |u_n|^2 \rangle, \qquad (3)$$

$$S_3(k_n) = \mathrm{Im}\{\langle u_{n-1}u_n u^*_{n+1}\rangle\}, \qquad (4)$$

$$S_4(k_n) = \langle |u_n|^4 \rangle, \qquad (5)$$

etc. Indeed, in [7] these objects were found in the inertial range to be close to the exact solution in thermodynamic equilibrium, which reads

$$S_2(k_n) = \frac{1}{B + A(a/c)^n}, \tag{6}$$

$$S_3(k_n) = 0, \tag{7}$$

$$S_4(k_n) = S_2(k_n)^2, \tag{8}$$

etc. Formula (6) has two asymptotes: for small n in agreement with energy equipartition, and for large n with enstrophy equipartition.

$$S_2(k_n) \sim k_n^0, \qquad n_L \ll n \ll n_c, \tag{9}$$

$$S_2(k_n) \sim \left(\frac{c}{a}\right)^n, \qquad n_c \ll n \ll n_f. \tag{10}$$

Here $n_c \approx \log(B/A)/\log(a/c)$ is the crossover shell separating the two asymptotic scaling forms of S_2. A and B are coefficients depending on the forcing and the dissipation. In particular, in this regime close to thermodynamic equilibrium, the crossover n_c moves to higher shells when the viscosity ν is reduced. Unless otherwise stated, we choose parameters such that $n_c \ll n_f$.

Equation (7) implies zero fluxes. However, in our simulations we find in this regime a finite inverse flux of energy and a direct flux of enstrophy which do not go to zero when $\gamma_n \to 0$. The fact that the fluxes do not vanish also implies that S_3 is not exactly zero. One can write down the exact form of S_3, which is correct always when there is a flux of energy or a flux of enstrophy:

$$S_3(k_n) \sim k_n^{-1}, \qquad n_L \ll n \ll n_f \text{ (energy flux)}, \tag{11}$$

$$S_3(k_n) \sim k_n^{-1}\left(\frac{c}{a}\right)^n, \qquad n_f \ll n \ll n_d \text{ (enstrophy flux)}. \tag{12}$$

The values of the energy flux $\bar{\epsilon}$ and the enstrophy flux $\bar{\eta}$ can be exactly evaluated, see [8]. In the two separate regimes (11) and (12) they read, respectively,

$$\bar{\epsilon} = k_n(c - a)S_3(k_n), \tag{13}$$

$$\bar{\eta} = k_n\left(\frac{a}{c}\right)^n(c - a)S_3(k_n). \tag{14}$$

These are constants in the corresponding ranges of k_n.

A measure of the deviation of the statistics from Gaussian behavior is provided by the skewness

$$R(k_n) \equiv \frac{S_3(k_n)}{S_2(k_n)^{3/2}}, \tag{15}$$

which according to Eqs. (6)–(12) has the three separate regimes

$$R(k_n) \sim k_n^{-1}, \qquad n_L \ll n \ll n_c, \tag{16}$$

$$R(k_n) \sim k_n^{-1}\left(\frac{a}{c}\right)^{3n/2}, \qquad n_c \ll n \ll n_f, \tag{17}$$

$$R(k_n) \sim k_n^{-1}\left(\frac{a}{c}\right)^{n/2}, \qquad n_f \ll n \ll n_d. \tag{18}$$

These regimes are illustrated in Fig. 1.

When R is small, it provides a measure of the magnitude of the fluxes compared to their standard deviations. R is of the order of unity at the dissipative boundaries, while it reaches its minimal value at $n = n_c$. The former follows from the fact that the dissipative boundaries are precisely where the second order dissipative terms balance the third order transfer terms. In fact, the ratio R cannot be larger than unity whenever scaling prevails. One sees this directly from the definitions (3) and (4):

$$S_3(k_n)/\sqrt{S_2(k_{n-1})S_2(k_n)S_2(k_{n+1})} \le 1. \tag{19}$$

Since n_c moves to higher shells when the viscosity is reduced, the value of R at the minimum decreases: we divide a decreasing S_3 by an S_2 that remains constant over a larger range of n. We thus conclude that the quasi-equilibrium regime displays an algebraic small parameter when $\nu \to 0$. We will see that in the Kolmogorov regime there is only a numerical small parameter.

In Ref. [7] it was then discovered that there exists a transition for b crossing a critical value ($b = -5/4$ for $\lambda = 2$), after which S_2 gains a new form in the direct enstrophy flux regime, close to the Kraichnan dimensional prediction

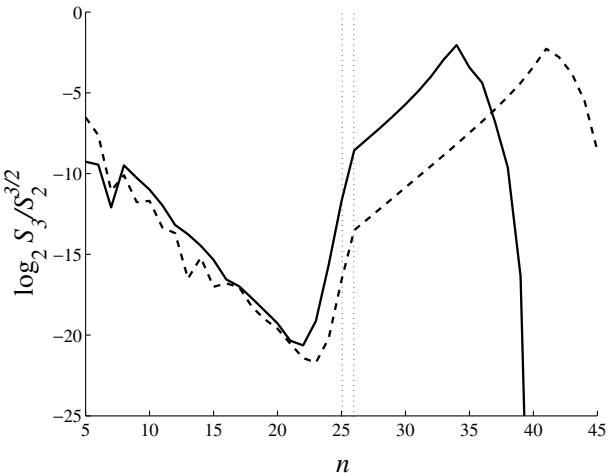

FIG. 1. The skewness $R(k_n) \equiv S_3(k_n)/S_2(k_n)^{3/2}$ as a function of n for $b = -1.1$ and $\nu = 10^{-43}$ (dashed line) and $\nu = 10^{-33}$ (solid line). One clearly sees the three regimes predicted by Eqs. (16)–(18), with the minimum occurring at $n = n_c$. The minimum deepens and moves to higher shells when the viscosity is reduced. The vertical dotted lines designate the forcing scale. Note that at small values of n the statistics converges on much longer time scales than for large values of n; hence the remnant fluctuations around the scaling prediction.

$$S_2(k_n) \sim k_n^{-2[1+\log_\lambda(a/c)]/3}, \qquad n_f \ll n \ll n_d \tag{20}$$

(up to small corrections). Exactly at $b = -5/4$ this coincides with the well-known k_n^{-3} prediction for the energy spectrum [1]. We note that this prediction can be inferred from the breakdown of Eq. (18) due to the condition (19). The latter condition means that R must be an *increasing* function of n towards its small scale boundary, where it attains its maximal value of the order of unity. This condition translates into the inequality

$$(a/c) \geq \lambda^2 \Leftrightarrow b \geq -a\left(1 + \frac{1}{\lambda^2}\right), \tag{21}$$

or $b \geq -5/4$ for $\lambda = 2$ and $a = 1$. Thus for $b < -5/4$ Eq. (18) can no longer be valid. While $S_3(k_n)$ does not change, $S_2(k_n)$ is replaced by the form (20), and consequently Eq. (18) is replaced by

$$R(k_n) \sim k_n^0, \qquad n_f \ll n \ll n_d (b < -5/4). \tag{22}$$

In Fig. 2 we present this ratio as computed from numerical simulations with the values of $b = -1.5$ and -1.6. We have used a total of 46 shells, with $\nu = 10^{-37}$, $\mu = 10^{-3}$. The forcing was on shells 15 and 16. The three regimes are clearly seen, with the added important confirmation that this ratio is always smaller than unity, approaching saturation of the bound at the viscous dissipative boundary.

Nevertheless, previous work failed to find a similar phenomenon for the range of scales that supports the inverse flux of energy. In that range the statistics remained close to thermodynamic equilibrium, leading to the common belief that shell models cannot be used to model two-dimensional turbulence. We explain next that the statistical solution claimed for the regime $b < -5/4$, i.e., local thermodynamic equilibrium for the inverse flux of energy and direct enstrophy cascade, predicts its own destruction when b is reduced further beyond a critical value b_c that we can compute analytically. Indeed, the set of Eqs. (16), (17), and (22), and the condition (19) further imply that R cannot be a decreasing function of n in the range $n_c \ll n \ll n_f$, which implies

$$\left(\frac{a}{c}\right)^{3/2} \geq \lambda \Leftrightarrow b \geq -a(1 + \lambda^{-2/3}). \tag{23}$$

Accordingly, for $b < b_c \equiv -a(1 + \lambda^{-2/3})$ the quasiequilibrium in the inverse energy flux regime can no longer be supported, and it changes into a true cascade regime with K41 scaling. For $\lambda = 2$ this occurs at the critical value $b_c \approx -1.63$, where $S_2(k_n)$ assumes the scaling form

$$S_2(k_n) \sim k_n^{-2/3}, \qquad n_L \ll n \ll n_f. \tag{24}$$

Note that Eq. (24) implies the collapse $n_c \to n_L$. In Fig. 3 we show the results of simulations at $b = -1.9$, with forcing at shells $n_f = 35, 36$ and otherwise the same parameter values as in Fig. 1. The agreement with K41 scaling is apparent. We note that the scaling laws (11) (which remains true in this regime) and (24) imply that $R(k_n)$ becomes constant as a function of k_n. Thus we cannot display an algebraic small parameter anymore. Nevertheless, the measurement of the constant value of R in the inverse cascade regime yields a number of the order of 0.02 or less. We thus have a *numerical* small parameter that is similar in magnitude to the corresponding value of R in two-dimensional turbulence [5].

In summary, we exhibited a new regime of the statistical properties of shell models in which inverse energy cascade exists side-by-side with a direct enstrophy cascade. The statistical objects satisfy scaling laws in close

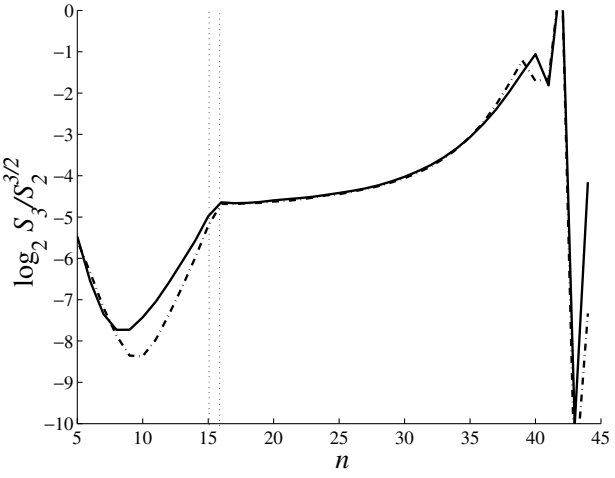

FIG. 2. Same as Fig. 1 but for $b = -1.5$ (dot-dashed line) and -1.6 (solid line). One clearly sees the three regimes predicted by Eqs. (16), (17), and (22). Note that the constant regime k_n^0 is still effected by finite size effects from the viscous end. However, the two curves are essentially the same.

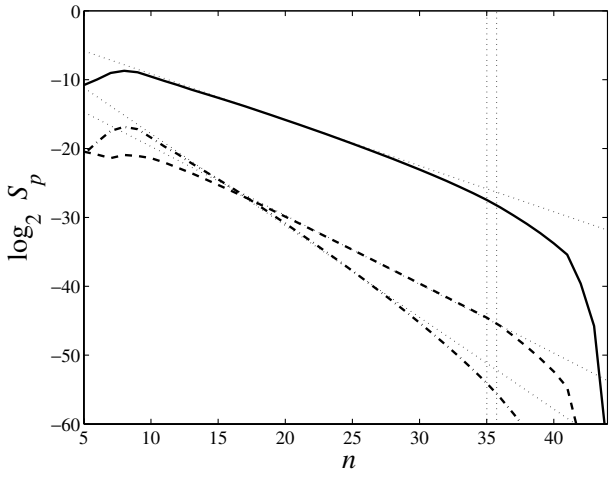

FIG. 3. Second (solid line), third (dashed line), and fourth (dot-dashed line) order structure functions in the inverse cascade regime for $b = -1.9$. The vertical dotted lines indicate the forcing range $n_f = 35, 36$. The dotted lines have K41 slopes of $-2/3$, -1, and $-4/3$, respectively.

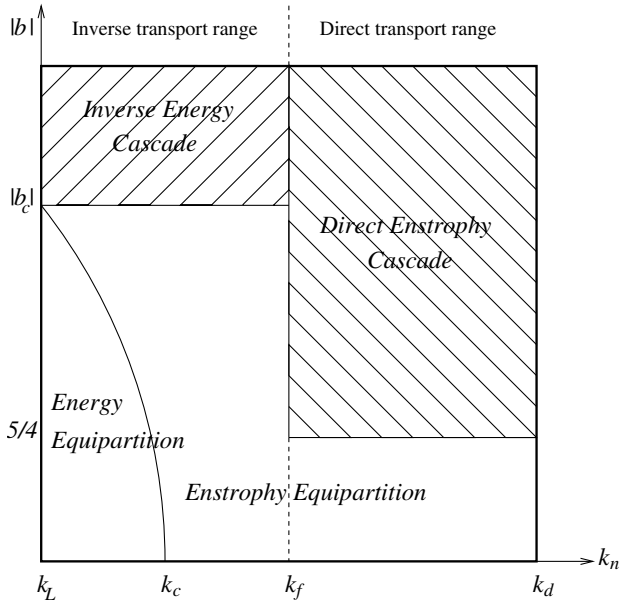

FIG. 4. Schematic phase diagram showing the different statistical steady states as a function of b and k_n. Note, in particular, that the inverse cascade regime is in the immediate proximity of a quasiequilibrium state with enstrophy equipartition.

correspondence with the Kraichnan dimensional predictions for two-dimensional turbulence. This statistical regime exists in proximity to a quasiequilibrium state. To clarify the situation we present in Fig. 4 a schematic phase diagram in which all the regimes are shown as a function of $|b|$ and k_n. We can perturb slightly the equilibrium state to create the inverse cascade with a small parameter. This will enable the study of the inverse cascade regime using perturbative techniques. Since the shell model is so much simpler than two-dimensional Navier-Stokes equations, it should provide useful grounds to understand the phenomenon theoretically. Such a discussion and a more detailed account of our numerical findings will be presented elsewhere [12].

This work has been supported in part by the European Commission under a TMR grant, the German Israeli Foundation, the Minerva Foundation, Munich, Germany, and the Naftali and Anna Backenroth-Bronicki Fund for Research in Chaos and Complexity.

[1] R. H. Kraichnan, Phys. Fluids **10**, 1417 (1967).
[2] P. Tabeling, Phys. Rep. **362**, 1 (2002).
[3] L. M. Smith and V. Yakhot, Phys. Rev. Lett. **71**, 352 (1993).
[4] J. Paret and P. Tabeling, Phys. Fluids **10**, 3126 (1998).
[5] G. Boffetta, A. Celani, and M. Vergassola, Phys. Rev. E **61**, R29 (2000).
[6] E. Aurell, G. Boffetta, A. Crisanti, P. Frick, G. Paladin, and A. Vulpiani, Phys. Rev. E **50**, 4705 (1994).
[7] P. D. Ditlevsen and I. A. Mogensen, Phys. Rev. E **53**, 4785–4793 (1996).
[8] V. S. L'vov, E. Podivilov, A. Pomyalov, I. Procaccia, and D. Vandembroucq, Phys. Rev. E **58**, 1811 (1998).
[9] T. Bohr, M. H. Jensen, G. Paladin, and A. Vulpiani, *Dynamical Systems Approach to Turbulence* (Cambridge University Press, Cambridge, United Kingdom, 1998), and references therein.
[10] E. B. Gledzer, Dokl. Akad. Nauk SSSR **209**, 1046 (1973) [Sov. Phys. Dokl. **18**, 216 (1973)].
[11] M. Yamada and K. Ohkitani, Phys. Rev. Lett. **60**, 983 (1988).
[12] T. Gilbert, V. S. L'vov, A. Pomyalov, and I. Procaccia (to be published).